International Journal of Biochemistry and Cell Biology 111 (2019) 63–71

Contents lists available at ScienceDirect

International Journal of Biochemistry and Cell Biology

journal homepage: www.elsevier.com/locate/biocel

MicroRNA-137 inhibits autophagy and chemosensitizes pancreatic cancer cells by targeting ATG5

Zhi-Chao Wang[a], Fei-Zhou Huang[a], Hong-Bo Xu[b], Ji-Chun Sun[a], Chang-Fa Wang[a,*]

[a] Department of Hepatobiliary and Pancreatic Surgery, The Third Xiangya Hospital of Central South University, Changsha, 410013, PR China
[b] Department of Surgery, The Third Xiangya Hospital of Central South University, Changsha 410013, PR China

ARTICLE INFO

Keywords:
ATG5
Autophagy
Chemosensitivity
miR-137
PC

ABSTRACT

Purpose: Autophagy play an important role in tumor chemotherapy resistance. It has been reported that miR-137 expression was reducedand involved in the regulation of sensitivity of PC cells to chemotherapy. However, little is known about the underlying molecular mechanisms. In this study, we hypothesized that miR-137 might sensitize PC cells to chemotherapy thought regulating cell autophagy.

Methods: Cell survival was determined with MTT assay. Apoptotic cells were assessed with flow cytometric analysis. Fluorescence intensity of GFP-LC3 and RFP-GFP-LC3 were examined with immunofluorescence analysis to determine the autophagy and autophagic flux level. Western blotting assay was used to determine protein expression levels of LC3II/LC3I, P62, FUNDC1 and ATG5. mRNA expression level of miR-137 was detected by reverse transcription-quantitative polymerase chain reaction (RT-qPCR). Dual-luciferase reporter assay was used to evaluate the directly binding of miR-137 with its targets. Xenograft model was setup to evaluate tumor growth.

Results: The results showed that doxorubicin (Dox) induced autophagy but downregulated the expression level of miR-137 in pancreatic cancer (PC) cells. In turn, overexpression of miR-137 enhanced the effect of Dox on decreasing cell survival, inducing cell apoptosis and inhibiting autophagy rather than influencing autophagic flux in PC cells. Further mechanistic study identified that ATG5 was a direct target of miR-137. Moreover, overexpression of ATG5 dramatically reversed the promotion of apoptosis and inhibition of autophagy mediated by higher expression level of miR-137. We also demonstrated that miR-137 sensitized PANC-1 cells to Dox through inhibiting ATG5 and autophagy *in vivo*.

Conclusions: Our findings demonstrated for the first time that miR-137 was able to promote sensitivity of PC cells to chemotherapy via inhibition of autophagy mediated by ATG5. Therefore, miR-137 may act as a potential therapeutic target for pancreatic cancer.

1. Introduction

Pancreatic cancer is one of the most devastating malignancies of the gastrointestinal tract. Pancreatic cancer is usually detected at an advanced stage, so only 10–20% of patients are resectable when first diagnosed. Systemic combination chemotherapy for advanced PC patients is the main treatment and therapy (Rosenberg and Mahalingam, 2018). However, high mortality rates remain a serious concern of PC pateints. The main reason of the poor prognosis is the resistance to standard chemotherapy in PC cells (Zhang et al., 2018a). Thus, development of new therapies for PC is urgently needed.

Autophagy was firstly reported in 1962 by Ashford and Porter (Levine and Kroemer, 2008). It is the sequential process by which the cytoplasmic components are engulfed by a phagophore, isolated in autophagosome, and broken down in the lysosome (Yan et al., 2016). Cytotoxic and metabolic stress, including nutrient starvation, growth factor depletion and hypoxia, can activate autophagy for maintaining cellular biosynthesis (Ruocco et al., 2016). Accumulating evidences have revealed that autophagy protect cancer cells from stressful conditions, which is an important reason for the chemoresistance of cancer cells (Huang et al., 2016; Xu et al., 2017; Zhu et al., 2018; Wiedmer et al., 2017). Therefore, combination treatment with autophagy inhibitors may be useful in sensitizing PC cells to chemotherapeutic treatment.

MicroRNAs (miRNAs) are small non-coding RNA molecules that negatively regulate gene expression by interacting with the 3′

* Corresponding author at: Department of Hepatobiliary and Pancreatic Surgery, The Third Xiangya Hospital of Central South University, No.138, Tongzipo Road, Yuelu District, Changsha, 410013, Hunan Province, PR China.
E-mail address: wangchangfa623@163.com (C.-F. Wang).

https://doi.org/10.1016/j.biocel.2019.01.020
Received 23 July 2018; Received in revised form 29 December 2018; Accepted 29 January 2019
Available online 30 January 2019
1357-2725/

untranslated region of targeted mRNA, leading to gene silencing (Liu et al., 2013). Dysregulation of miRNAs expression has been shown to regulate the sensitivity to anticancer agents in various types of cancers (Chen et al., 2018; Sun et al., 2018; Min et al., 2015). Notably, miRNAs as new players were found to function in the regulation of autophagy in terms of induction, vesicle nucleation, elongation, autophagosome maturation and lysosome fusion (Gozuacik et al., 2017). MiR-137 has been demonstrated as a tumor suppressor in many kinds of human malignancies (Li et al., 2017). In addition, miR-137 has been shown to inhibit tumor growth and sensitizes chemosensitivity in lung cancer (Shen et al., 2016) and neuroblastoma cells (Takwi et al., 2014). More importantly, it was reported that miR-137 inhibited mitophagy via regulation of two mitophagy receptors FUNDC1 and NIX (Li et al., 2014). miR-137 upregulation prevents autophagy in glioma cells, whereas its antagomir promotes augophagy (Zeng et al., 2015). Previous reports suggested that miR-137 expression is reduced in human pancreatic tumors and regulated PC cells tumor growth, invasion and sensitivity to chemotherapy (Neault et al., 2016; Xiao et al., 2014), suggesting that miR-137 is able to potentiate the chemotherapy. However, the mechanism of action remains under investigation.

In the present study, we demonstrated that Dox-induced autophagy decreases the level of miR-137. In turn, miR-137 enhanced chemosensitivity via inhibition of autophagy. Our findings provide new insights into the molecular mechanism of PC chemoresistance as well as provide new therapeutic strategy for PC treatment in the future.

2. Materials and methods

2.1. Cell culture and treatment

Human PC cells PANC-1 were purchased from the American Type Culture Collection (VA, USA). The cells were grown in Dulbecco's Modified Eagle's Medium (DMEM, St. Louis, MO, USA) containing 10% FBS along with penicillin (100 units/mL) and streptomycin (100 μg/mL) at 37 °C in a humidified atmosphere of 5% CO2. Cells were grown 24 h to reach to 80% confluency followed by treatment with Doxorubicin (Dox), Rapamycin and 3-MA (Sigma Aldrich, St Louis, MO, USA) as shown in the figure legends.

2.2. Generation of Doxorubicin (Dox) resistant cells

For generation of Dox resistant PANC-1 cells (PANC-1-Dox), PANC-1 cells were seeded at a density of 3×10^5 in two 25 cm^2 flasks. One flask was left untreated but was passaged alongside the treatment flask, in which the cells were continuously treated with gradually increasing dose of Dox. After 5 months of Dox conditioning, the sensitivity of the cells was tested.

2.3. Cell transfection and infection

Transfection was performed with Lipofectamine® 2000 (Thermo Fisher Scientific, Inc.) according to the manufacturer's protocols. The ATG5 cDNA was subcloned into the multicloning site of the pCMV vector. The inserted region of the constructs was verified by DNA sequencing. To establish PANC-1/GFP-LC3 and hsa-miR-137 stable cell lines, proliferating PANC-1 cells were transfected with GFP-LC3 and hsa-miR-137 lentiviral plasmid. The oligonucleotides of hsa-miR-137 mimic and its non-specific control were synthesized by Genepharma (Shanghai, China) and were then amplified and cloned into lentiviral vectors. Lentivirus carrying GFP-LC3 or hsa-miR-137 was packaged according to the manufacturer's manual. The lentiviral packaging kit was purchased from Open Biosystems (Huntsville, AL, USA). Lentivirus were packaged in HEK293 T cells and collected from the medium supernatant. Stable cell lines were established by infecting lentivirus into PANC-1 cells and selected by puromycin.

2.4. Cell viability assay

Cell survival was determined by 3-(4,5-dimethylthiazol-2-yl)-2,5-diphenyltetrazolium bromide (MTT, Sigma, St. Louis, MO, USA) assay, which is a colorimetric assay for assessing cell metabolic activity. Viable cells with active metabolism convert MTT into a purple colored formazan product, thus color formation serves as a useful and convenient marker of only the viable cells. Briefly, the cells at log-phase were seeded in 96-well plates at 3×10^3 cells per well. After 24 h incubation, 20 μl sterile MTT was added into each test well in triplicates. After 4 h continuous culture, the supernatant was completely removed, with the addition of 150 μl dimethyl sulfoxide (DMSO, Sigma, St. Louis, MO, USA) for 10 min vortex until the complete resolving. The absorbance of each sample was measured at 570 nm.

2.5. Annexin V-FITC/PI staining

To assess the quantification of apoptotic cells, 5×10^6 cells were harvested and resuspend in 100 μl 1 x Annexin V binding buffer. The cells were stained with 10 μl Annexin V-FITC and PI and incubate tubes in the dark for 15 min at room temperature according to the protocol of Apoptosis Detection Kit (BD Pharmingen). The percentage of apoptotic cells was determined by flow cytometry (BD Biosciences) and analyzed by FlowJo 7.6 (Ashland, OR, USA).

2.6. Autophagy assay

Autophagy was assayed by light microscopic quantification of fluorescent autophagosomes in cells transfected with GFP-LC3. Cells were cultured in DMEM with 10% fetal calf serum prior to analysis. The formation of GFP fluorescent puncta was observed under fluorescence microscopy. The number of GPF-LC3 puncta per GFP-LC3 positive cell was assessed by counting a minimum of 50 cells for duplicate samples per condition in three independent experiments. The autophagic flux was measured by the monomeric red fluorescent protein (mRFP)-GFP-LC3 tandem reporter construct. Lentiviral was generated via calcium phosphate transfection of mRFP-GFP-LC3 plasmid. The lentiviral supernatant was added to PANC-1 cells with the supplement of Polybrene (5 mg/ml) for 6 h incubation. The cells were cultured in DMEM with 3 μg/ml puromycin for 2 weeks. And then, the stable PANC-1 cells were treated with Dox in the presence or absence of miR-137 or pCMV-ATG5. The GFP and RFP signals were observed under fluorescence microscopy.

2.7. Reverse transcription-quantitative polymerase chain reaction (RT-qPCR)

Total RNA was extracted from EC cell lines and normal/tumor paired tissues with TRIzol reagent (Invitrogen, Carlsbad, CA) according to the manufacturer's instructions. RNA of 2 μg was used to synthesize cDNA by using a first strand cDNA kit (Sigma, Munich, Germany), following to the manufacturer' protocol. PCR amplification was performed using a SYBR Green PCR kit (Thermo) and run on an ABI 7300 Thermocycler (Applied Biosystems, Foster City, CA, USA). The specific primers of were: ATG5, Forward: 5′-AAGACCTTCTGCACTGTCCA-3′, Reverse: 5′-GAGTTTCCGATTGATGGCCC-3′; FUNDC1, Forward: 5′-AAGACCTTCTGCACTGTCCA-3′, Reverse: 5′- GCTGCTTTGTTCGCTC GTTT'; miR-137, Forward: 5′- GCGCGCTTATTGCTTAAGAATAC-3′, Reverse: 5′- CGGCCCAGTGTTCAGACTAC-3′; U6, Forward: 5′- CTCGC TTCGGCAGCACA-3′, Reverse: 5′-AACGCTTCACGAATTTGCGT-3′; GAPDH, Forward: 5′-CCAGGTGGTCTCCTCTGA-3′, Reverse: 5′- GCTG TAGCCAAATCGTTGT-3′. The $2^{-\Delta\Delta Ct}$ method was used to calculate differences in mRNA expression.

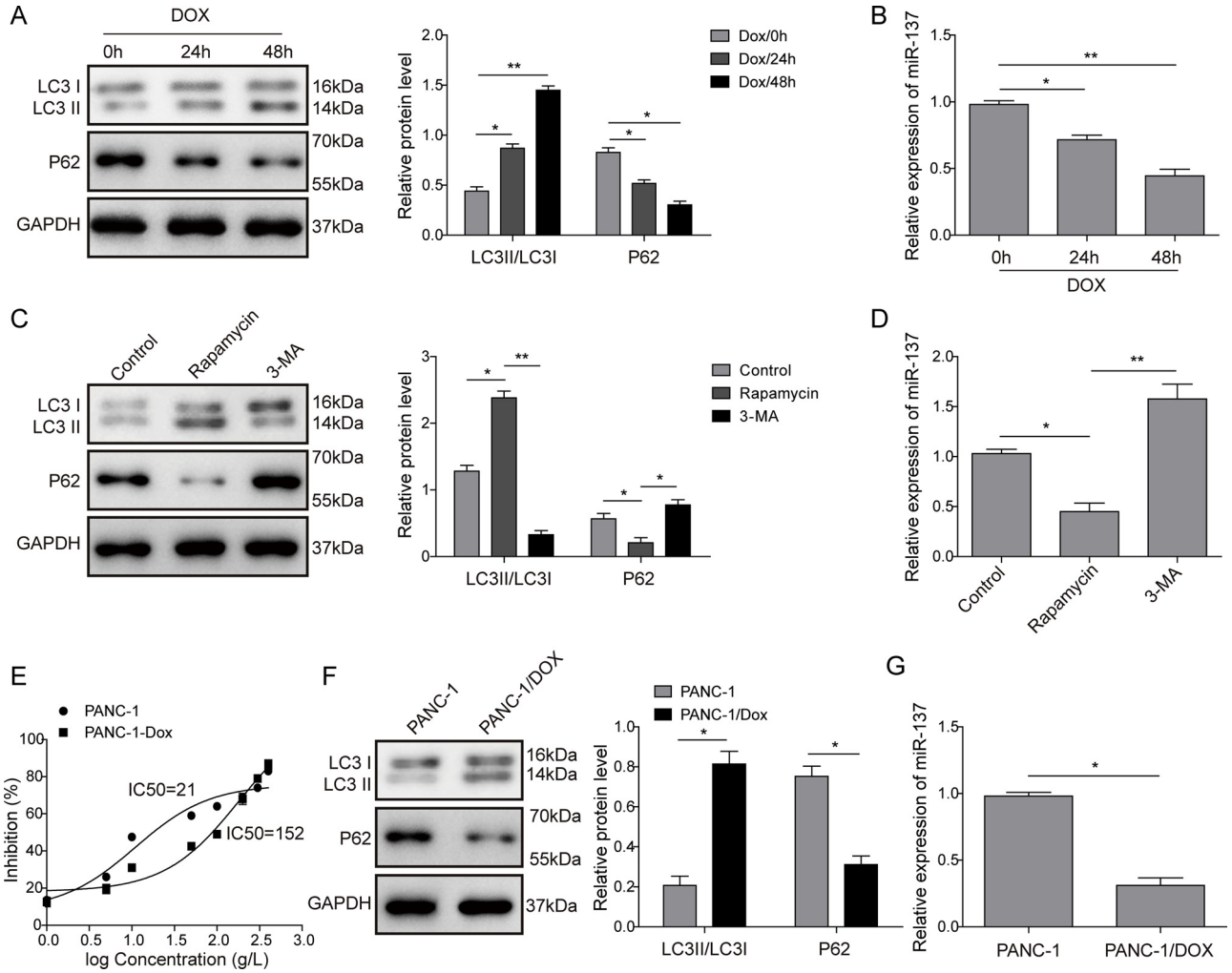

Fig. 1. Dox-induced autophagy decreases miR-137 levels. (A) western blotting analyses of P62, LC3-I and LC3-II in PANC-1 cells after treatment with Dox at 2 μg/ml for 24 and 48 h. (B) Relative levels of miR-137 in PC cells after treatment with Dox for 24 and 48 h were analyzed using RT-qPCR. (C) western blotting analyses of P62, LC3-I and LC3-II in PANC-1 cells after treatment with or without rapamycin (autophagy inducer) at 2 μM and 3-MA (autophagy inhibitor) at 10 mM for 24 h. (D) Relative levels of miR-137 in PC cells after treatment with or without rapamycin and 3-MA. (E) PANC-1 and PANC-1/Dox cells were incubated with Dox with concentration between 0–40 μg/ml for 48 h. Cell viability was evaluated with MTT assay. (F) western blotting analyses of P62, LC3-I and LC3-II in PANC-1 and PANC-1/Dox cells. (G) Relative levels of miR-137 PANC-1 and PANC-1/Dox cells. Data are expressed as the mean ± SD of 3 replicates. $^{*}P < 0.05$; $^{**}P < 0.01$.

2.8. Protein isolation and western blot analysis

Total protein of cells and tissues was extracted using RIPA Buffer (Cell Signaling Technology, Danvers, MA, USA). The protein concentration was assessed with a bicinchoninic acid (BCA) assay kit from EMD Millipore (Billerica, MA, USA). Protein was separated with 12% SDS polyacrylamide gel electrophoresis and transferred to electrotransferring onto PVDF membranes. Subsequently, the membrane was blocked in 5% nonfat milk for 1 h at room temperature and immunoblotted overnight at 4 °C with the antibodies. Then the membranes were incubated with secondary antibodies for 2 h at room temperature. The anti-glyceraldehyde 3-phosphate dehydrogenase (GAPDH) (#ab8245), LC3 (#ab51520), P62 (#ab56416), ATG5 (#ab221604), and FUNDC1 (#ab224722) antibody and secondary antibodies HRP-labeled goat anti-rabbit IgG (#ab7097) were purchased from Abcam (Cambridge, UK). Bands were developed using RapidStep™ ECL Reagent (EMD Millipore) according to the manufacturer's directions.

2.9. Dual-luciferase reporter assay

Luciferase reporter vectors were obtained cloning the full 3′UTR sequences of ATG5 or FUNDC1 downstream to the luciferase gene in pMIR-REPORT vector (Thermo Fisher, Waltham, MA, USA), respectively. The cells in 24-well plate were transfected with 80 ng of pMIR-REPORT plasmid construct, 8 ng of pRL-TK vector as internal reference, and 50 nM of double-stranded miRNA mimics. Forty-eight hours later, the activities of firefly and renilla luciferase were measured using Dual-Glo Luciferase Assay System (Promega) according to the manufacturer's instructions. The experiments were repeated for three times with triplicate in each group.

2.10. Tumor xenografts

Six-week-old female nude athymic BALB/c nu/nu mice were used for xenograft studies. PANC-1 or overexpression miR-137 PANC-1 cells (5×10^6) were resuspended in 100 μL of PBS and implanted subcutaneously into the bilateral flank region of the mice. The treatment of mice was carried out intravenously (through tail vein) once a week for 30 days (total of 4 applications) using 5 $\mu g \cdot g^{-1}$ of body weight of Dox. Tumor volume of each group was calculated by caliper every 5 days. The volume of the tumor was calculated following the formula: volume = 1/2 × length × width^2. The mice were killed after 30 days later and the tumors were dissected out. All experimental procedures

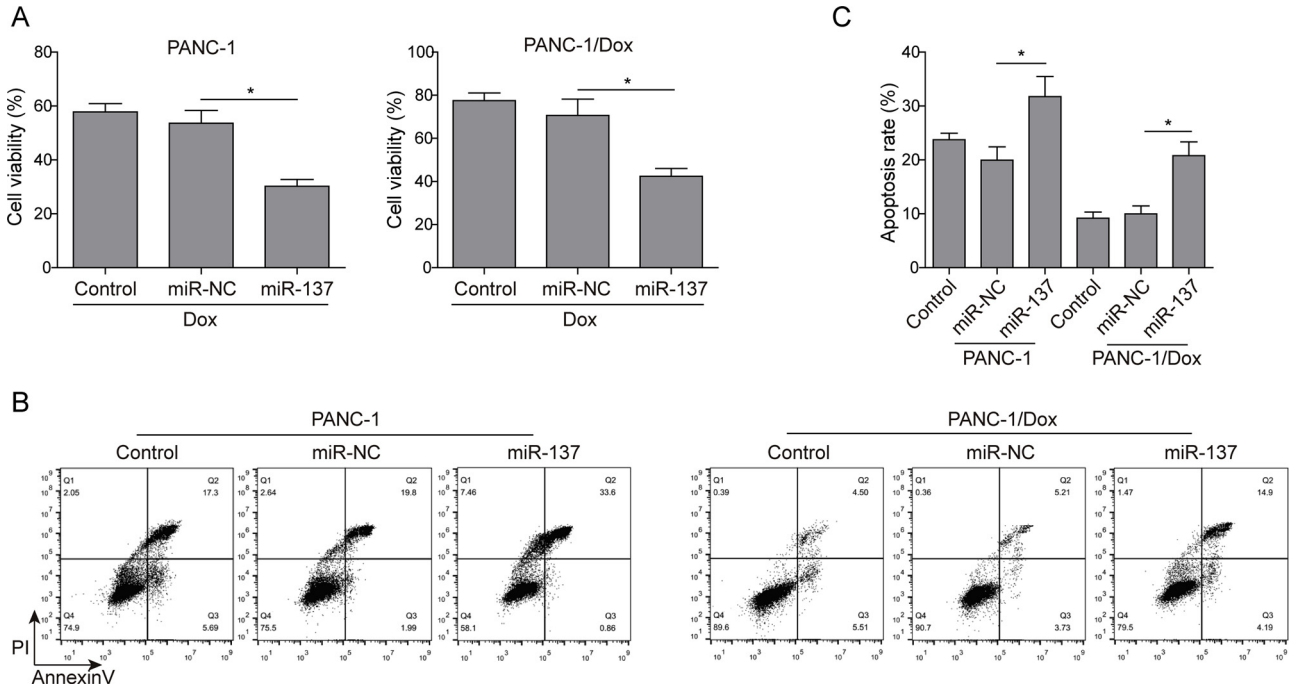

Fig. 2. miR-137 enhanced Dox sensitivity to PC cells. (A) PANC-1 and PANC-1/Dox cells were treated with Dox at 2 μg/ml and 12 μg/ml for 48 h, respectively. The cell viability was determined with MTT assay. (B) Cell apoptosis was determined with cell flow cytometric assay. PANC-1 and PANC-1/Dox cells were treated with Dox at 2 μg/ml and 12 μg/ml for 24 h, respectively. Data are expressed as the mean ± SD of 3 replicates. *$P < 0.05$; **$P < 0.01$.

involving animals were performed in accordance with "Principles of Laboratory Animal Care" (NIH publication no. 85-23, revised 1985). And the experiments were performed with the approval of the Ethics Commission at the 3rd Xiangya Hospital of Central South University.

2.11. Statistical analysis

Statistical analysis was performed with the SPSS statistical software program (version 13.0; SPSS, Inc., Chicago, IL, USA). Differences between groups were determined with the Student *t*-test or oneway ANOVA. The Student *t*-test was used for the analysis of independent two groups. Oneway analysis of variance with the post hoc Tukey test was used for the analysis of difference among three or more groups. $P < 0.05$ was considered statistically significant ('*' represents $P < 0.05$, '**' represents $P < 0.01$). All data were presented as the mean of at least triplicate samples ± standard deviation.

3. Results

3.1. Dox-induced autophagy decreases the level of miR-137

To confirm whether autophagic activity is altered by Dox treatment, LC3 II /LC3 I protein level was examined upon treatment of Dox at 2 μg/ml. Western blotting showed that the Dox time-dependently induced progression of LC3-I to LC3-II and downregulation of p62 protein level (Fig. 1A). Simultaneously, RT-qPCR showed that Dox decrease mRNA expression levels of miR-137 over time (Fig. 1B). To determine whether autophagy modulated expression level of miR-137, cells were treated with the autophagy inducer rapamycin (2 μM) and autophagy inhibitor 3-MA (10 mM), respectively. The regulatory effect of the two compounds on cell autophagy was confirmed by western blot assay (Fig. 1C). In parallel, rapamycin significantly inhibited expression of miR-137 while 3-MA increased its expression (Fig. 1D). Additionally, the Dox-resistant cell line PANC-1/Dox was generated, which was about 7.5-fold more resistant than its parental cell line (Fig. 1E). PANC-1/Dox cells showed higher protein level of LC3-II/LC3 I and lower protein level of P62 (Fig. 1F). The expression level of miR-137 was lower in PANC-1/Dox cells relative to that of PANC-1 cells (Fig. 1G). These findings indicate that Dox-induced autophagy decreases the level of miR-137 in PANC-1 cells.

3.2. miR-137 enhanced Dox sensitivity of PC cells

Next, the effect of miR-137 on the activity of Dox was evaluated. Overexpression of miR-137 dramatically sensitized the PC cells to Dox, with cell survival rate decreased from 51% to 30% in PANC-1 cells (Fig. 2A). Consistently, overexpression of miR-137 remarkably inhibited cell survival in PANC-1/DOX (Fig. 2B). Moreover, overexpression of miR-137 potentiated Dox-induced cell apoptosis, with increase from about 20% to 31% in PANC-1 cells and from 10% to 20% in PANC-1/Dox cells, respectively (Fig. 2C). These data indicate that miR-137 promoted Dox activity in PC cells.

3.3. miR-137 decreased the resistance of PC cell to Dox through downregulating autophagy

To understand the mechanism underlying the effect of miR-137 on Dox sensitivity in PC cells, we hypothesized that miR-137 potentiated the sensitivity of Dox to PC cells through regulating cell autophagy. To test this hypothesis, PANC-1/GFP-LC3 cells were treated with Dox in the presence or absence of miR-137 expression. Treatment of cells with Dox alone induced the number of punctate GFP-LC3. However, expression of miR-137 antagonized the effect of Dox on the number of punctate GFP-LC3 (Fig. 3A and B). Autophagy is a continuous process, and autophagic flux requires both autophagosome synthesis and their subsequent degradation at lysosomes. We further used the RFP-GFP-LC3 construct to differentiate between autophagosomes and autolysosomes. Dox treatment increased the numbers of RFP-LC3-labeled puncta and yellow puncta, indicating Dox induced complete autophagy in PANC-1 cells. However, expression of miR-137 reversed the effect of Dox on the number of yellow color-labeled autophagosome while showed no significant effect on Dox induced green puncta (Fig. 3C). These results demonstrate that miR-137 had a defect in the formation of autophagosomes, rather than in the fusion of autolysosomes not

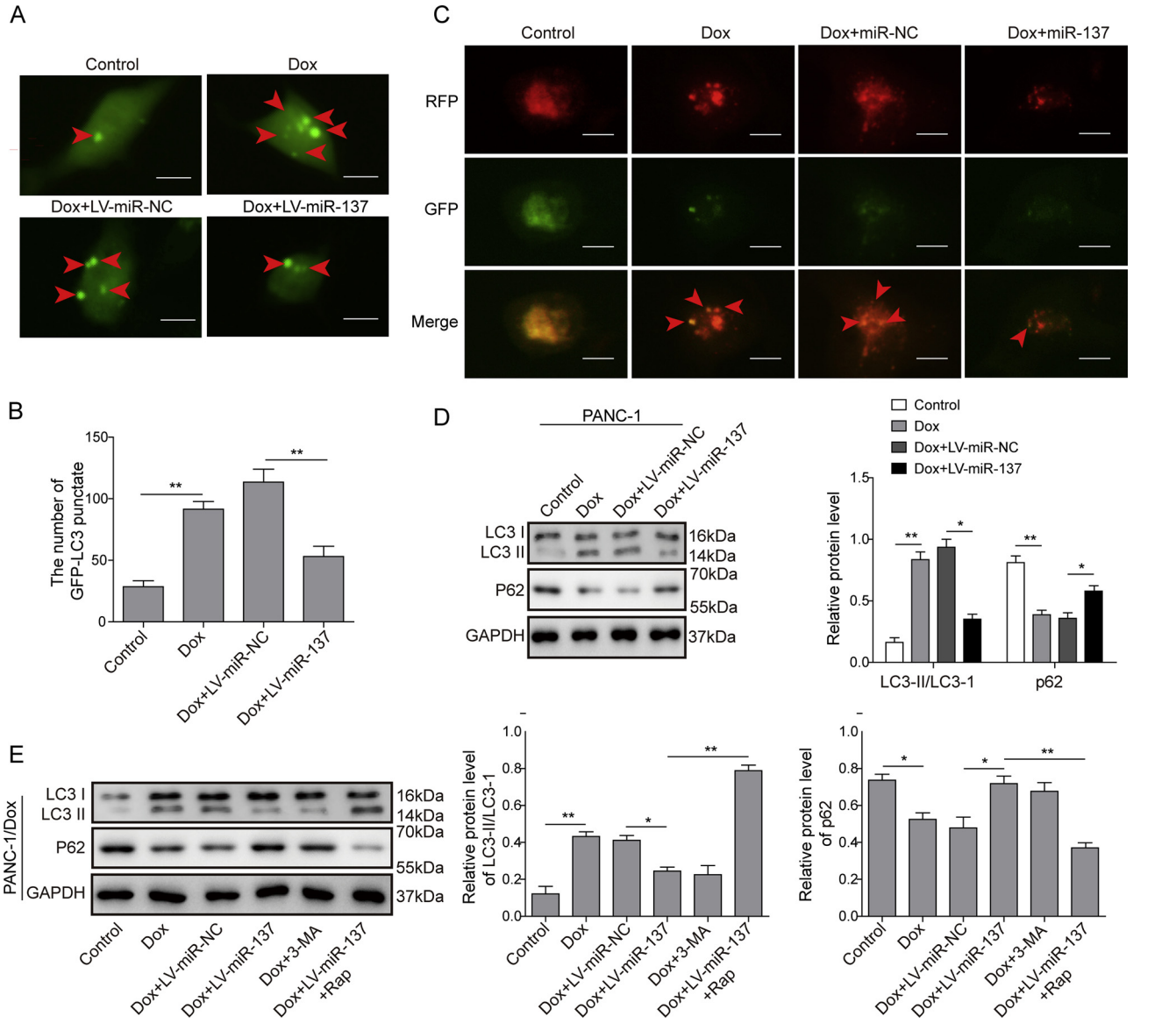

Fig. 3. miR-137 decreased the resistance of PC cell to Dox through downregulating autophagy. (A and B) PANC-1 stably expressing GFP-LC3 cells were treated with Dox(2 μg/ml)in the presence or absence of miR-137 expression followed by observation to count GFP-LC3 puncta. 50 cells/ group were counted. Scale bar: 50 μm. (C) PANC-1 RFP-GFP-LC3 tandem reporter cells were treated with Dox in the presence or absence of miR-137 expression followed by Fluorescence Microscopy analysis. (D) PANC-1 cells were treated with Dox in the presence or absence of miR-137 expression followed by western blotting analyses of P62, LC3-I and LC3-II. (E) PANC-1/Dox cells were infected with LV-miRNA-NC, LV-miR-137; after 24-htransfection, cells were treated with 3-MA (10 mM) or rapamycin (2 μM) for a further 24 h before western blotting analyses of P62, LC3-I and LC3-II. Data are expressed as the mean ± SD of 3 replicates. *$P < 0.05$; **$P < 0.01$.

affected. In addition, Dox treatment robustly induced the progression of LC3-I to LC3-II and decrease in P62 expression, which is abolished with miR-137 expression in PANC-1 and PANC-1/Dox cells (Fig. 3D and 3E). In addition, similar with 3-MA treatment, inhibition of autophagy by miR-137 abolished the effect of Dox in PANC-1/Dox cells, and rapamycin treatment reversed the inhibitory effect of miR-137 overexpression on Dox-induced autophagy (Fig. 3E).

3.4. ATG5 is a downstream target of miR-137 in PC cells

In order to identify the potential targets of miR-137, two prediction softwares (microRNA.org and starbase) were used for prediction. We identified two genes closely related with autophagy, FUNDC1 and ATG5, predicted to be targeted by miR-137 (Fig. 4A). Next, we confirmed that endogenous mRNA and protein levels of ATG5 but not FUNDC1 was downregulated in miR-137-transfected PANC-1 cells (Fig. 4B and C). Conversely, knockdown of miR-137 inhibited the mRNA and protein levels of ATG5 (Fig. 4B and C). Luciferase reporter assay showed that exogenous miR-137 in PANC-1 cells exerted repressive effects on luciferase activity of wild-type ATG5 3′-UTR vectors but not FUNDC1, and inhibition of miR-137 resulted in an increased luciferase activity (Fig. 4D). When mutations were introduced into the potential 3′-UTR miR-137 binding sites, the mutation in ATG5 but not FUNDC1 prevented the downregulation of reporter activities by miR-137 (Fig. 4D). Moreover, Dox treatment decreased the mRNA and protein level of ATG5 over time (Fig. 4E and F), verifying that the suppressive effects of miR-137 showed direct interaction with binding sites in the ATG5.

3.5. miR-137 inhibited autophagy and potentiated sensitivity of Dox to PC cells via targeting ATG5

We further speculated that miR-137 may prevent autophagy and increase the sensitivity of PC cells to Dox by targeting ATG5. As shown

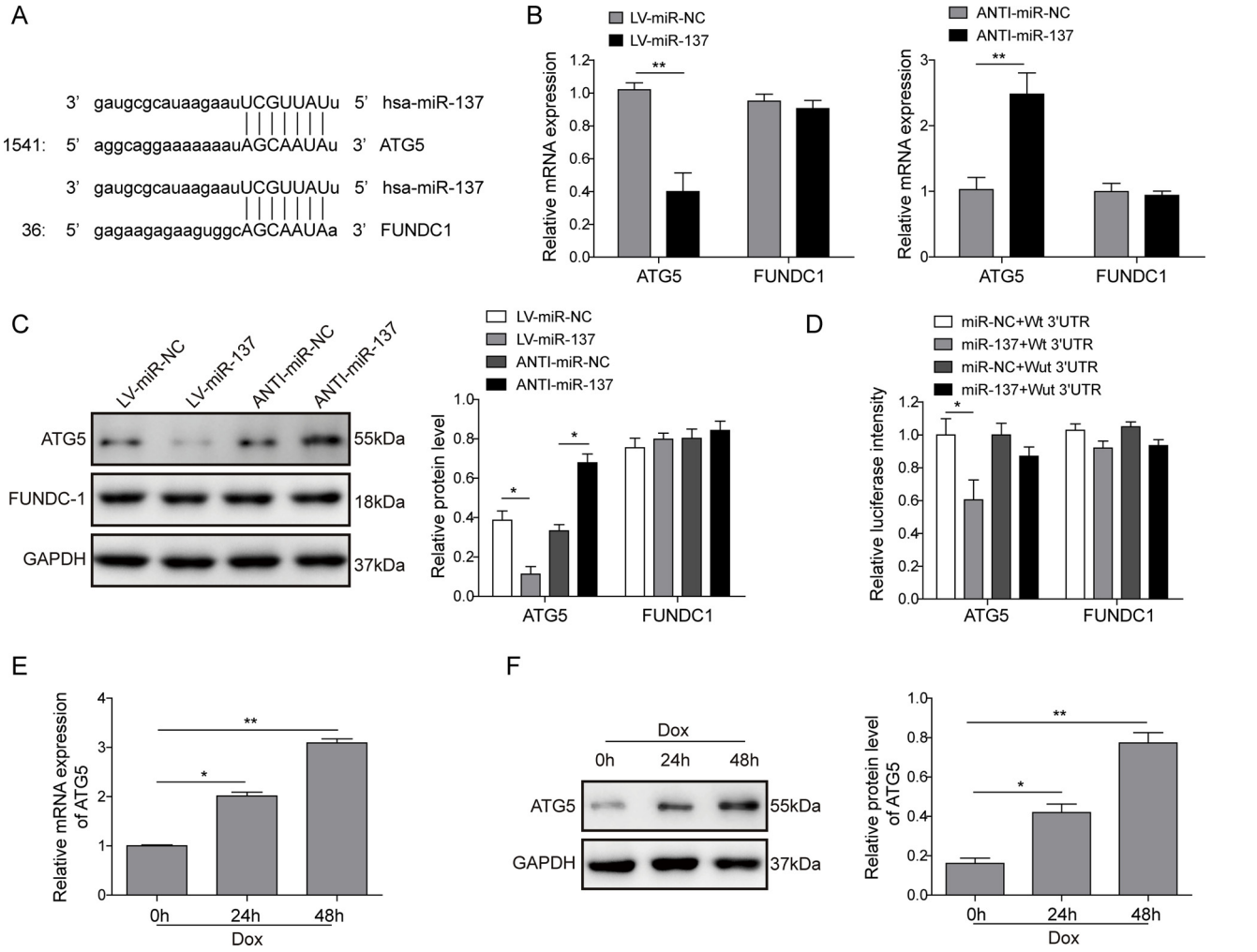

Fig. 4. MiR-137 directly targets ATG5. (A) A schematic diagram of ATG5 and FUNDC1 3′-UTR as a putative target for miR-137. The seed-recognizing sites in the 3′-UTR by miR-137 are indicated. (B) Relative mRNA expression of ATG5 and FUNDC1 upon overexpression or inhibition of miR-137. (C) Protein level of ATG5 and FUNDC1 upon overexpression or inhibition of miR-137. (D) Relative luciferase activity in HEK293T that were transfected with firefly luciferase reporters containing wildtype or mutant 3′-UTRs of ATG5 and FUNDC1, miR-137 or miR-NC. (E and F) mRNA and protein level of ATG5 in PC cells treated with Dox for 24 and 48 h. Data are expressed as the mean ± SD of 3 replicates. $^{*}P < 0.05$; $^{**}P < 0.01$.

in Fig. 5A, miR-137 decreased the number of punctate GFP-LC3 induced by Dox, whereas ATG5 overexpression increased the number of punctate GFP-LC3. When PANC-1 cells were co-transfected with miR-137 expression plasmid LV-miR-137 and ATG5-expressing plasmid pCMV-ATG5, the effect of ATG5 on Dox treatment was largely abolished (Fig. 5A). Similarly, the data also showed that expression of miR-137 inhibited the yellow color-labeled autophagosome while ATG5 overexpression enhanced the autophagosome numbers and obvious reversed the effect of miR137 (Fig. 5B). Moreover, miR-137 decreased ATG-5 and LC3-II/ LC3-I protein expression, and increased in P62 expression that were induced by Dox, whereas ATG5 overexpression increased AGT5 and LC3-II/ LC3-I expression, and decreased in P62 expression that were induced by Dox, which was reversed when PC cells were co-transfected with LV-miR-137 and pCMV-ATG5 plasmids (Fig. 5C). Furthermore, overexpression of ATG-5 suppressed Dox-induced cell apoptosis and reversed the promotion of apoptosis by miR-137 (Fig. 5D). Furthermore, overexpression of ATG-5 enhanced cell resistance to Dox, whereas co-transfection with LV-miR-137 and pCMV-ATG5 plasmids abolished the effect of ATG-5 on cell viability (Fig. 5E). Collectively, miR-137 prevents the autophagy and increases the sensitivity of PC cells by targeting ATG5.

3.6. miR-137 sensitized PANC-1 cells to Dox through decreasing ATG5 and autophagy in vivo

Next, we evaluated whether miR-137 enhance the ability of Dox to block the growth of tumors by targeting autophagy *in vivo*. The animals were implanted with PANC-1 overexpression miR-137 stable cells or control cells and injected Dox or PBS. The results showed that neither Dox nor miR-137 treatment alone was active, whereas the combination of miR-137 and Dox can significantly decrease tumor burden in terms of tumor volume (Fig. 6A and B), mass of tumor (Fig. 6C) compared with control group. Next, we investigated whether the effect of miR-137 in sensitizing tumor cells to Dox was mediated by inhibition of autophagy. Overexpression of miR-137 or Dox treatment significantly increased or decreased the level of miR-137 in the tumor, respectively. Overexpression of miR-137 largely abolished the inhibitory effect of Dox (Fig. 6D). Western blotting analysis showed that Dox administration significantly induced decrease in P62 protein expression, increase in ATG5 protein expression and higher transfer of LC3-I to LC3-II in tumors whereas tissues from the miR-137 group exhibited higher P62 expression and lower ATG5 expression and decreased transfer of LC3-I to LC3-II than control group, while combination of miR-137 and Dox restore the effect of Dox (Fig. 6E).

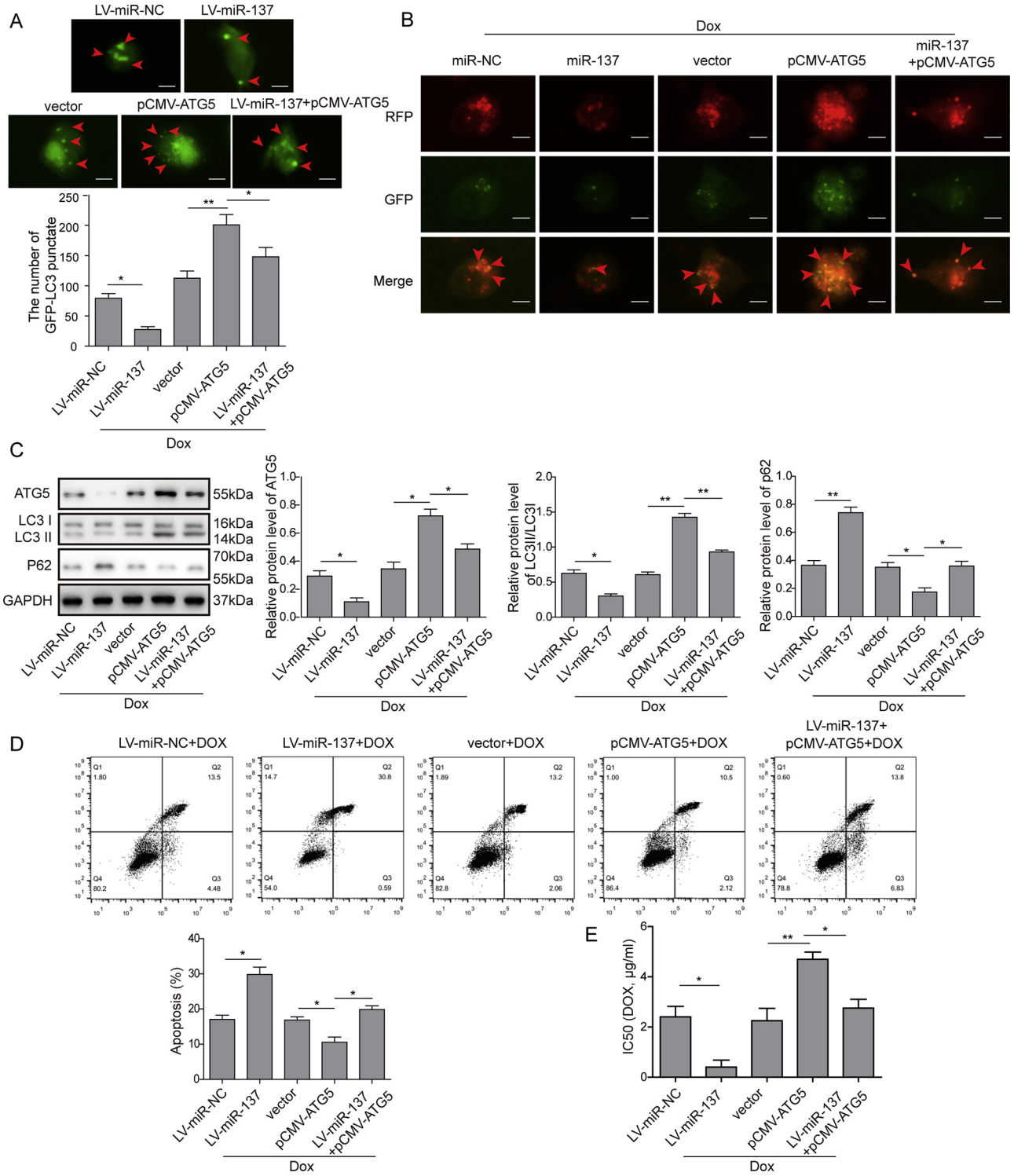

Fig. 5. miR-137 inhibited autophagy and potentiated sensitivity of Dox to PC cells via targeting ATG5. (A) PANC-1 stably transfected with GFP-LC3 cells were overexpressed with LV-miR-NC, LV-miR-137, vector control or LV-miR-137 plus ATG5-expressing plasmids and cotreated with Dox at 2 μg/ml, followed by observation to count GFP-LC3 puncta. Scale bar: 50 μm. (B) PANC-1 mRFP-GFP-LC3 tandem reporter cells were overexpressed with miR-NC, miR-137, vector control or miR-137 plus ATG5-expressing plasmids and cotreated with Dox at 2 μg/ml, followed by fluorescence microscopy analysis. (C) Western blotting analyses of P62, LC3-I and LC3-II. (D) Cell apoptosis was evaluated with cell flow cytometric analysis. (E) IC50 was determined with MTT assay. Data are expressed as the mean ± SD of 3 replicates. $^{*}P < 0.05$; $^{**}P < 0.01$.

4. Discussion

Pancreatic cancer is one of the most devastating malignancies of the gastrointestinal tract as well as one of the most common causes of cancer-associated mortality worldwide. For most patients with pancreatic cancer, chemotherapy often remains the last treatment option (Sato-Dahlman et al., 2018). Resistance to first-line chemotherapeutic drugs contributes to the poor prognosis of patients with pancreatic cancer (Chin et al., 2018). Previous study showed that miR-137 was able to markedly increased sensitivities to chemotherapy, but the

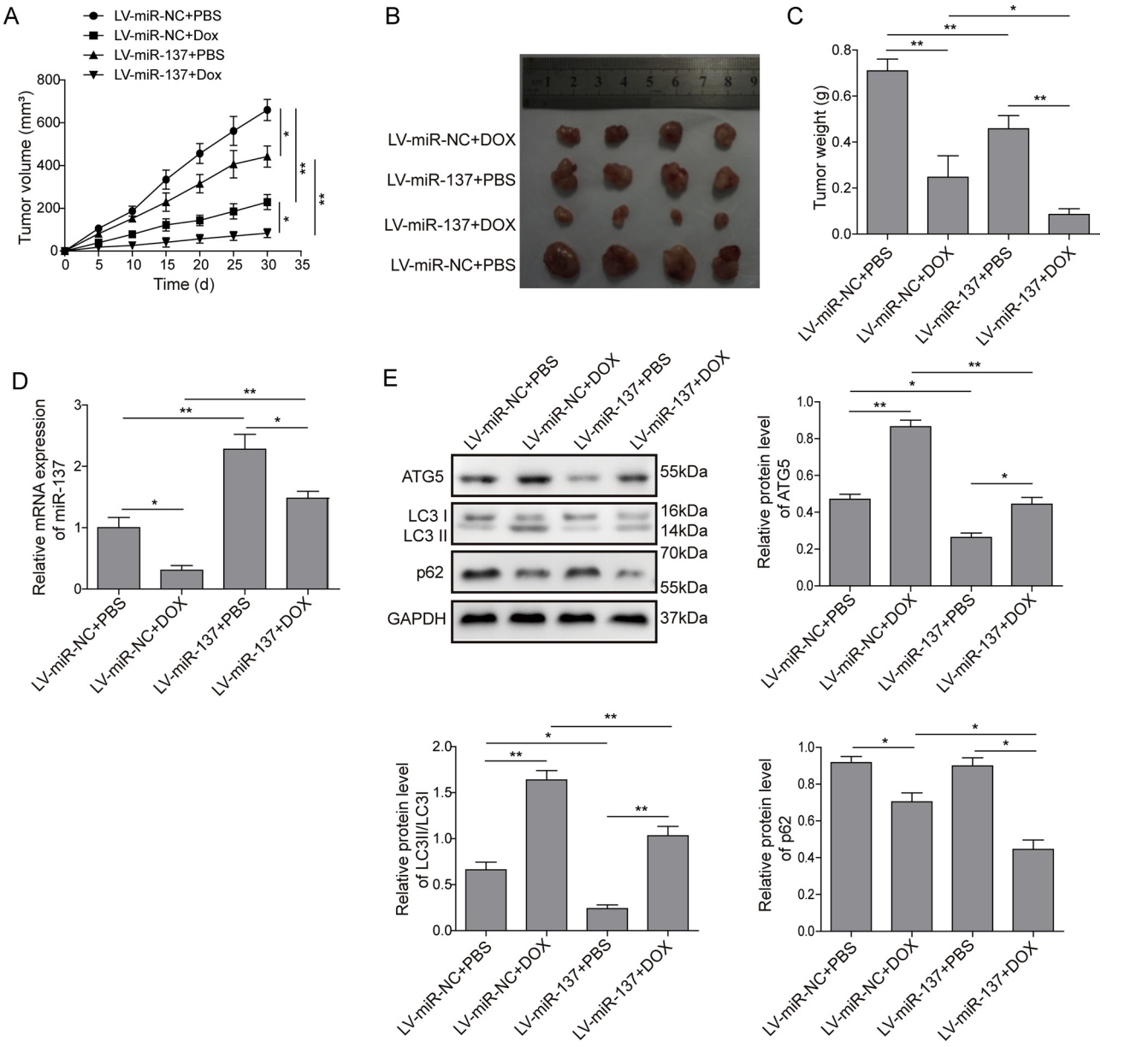

Fig. 6. Overexpression of miR-137 enhance the efficiency of Dox by inhibiting autophagy *in vivo*. PANC-1 overexpressing miR-137 stable cells or control cells were intravenously implanted into the tail of six-week old nude mice and were randomly grouped into four groups with 4 mice per group. Animals were i.v. dosed with Dox or vehicle as described in the method. Three independent experiments were conducted. (A) Tumor growth curve. (B and C) The quantitative analysis of tumor volume and weight. (D) Quantitative analysis of miR-137 levels in tumors and livers of four mouse groups. (E) western blotting analyses of P62, LC3-I and LC3-II in the tumors and livers of mice. Data are expressed as the mean ± SD $^{*}P < 0.05$; $^{**}P < 0.01$.

underlying molecular mechanisms are poorly characterized (Xiao et al., 2014). The results of the present study showed that Dox induced autophagy decrease the expression level of miR-137 in PC cells. In turn, overexpression of miR-137 enhanced the ability of Dox to inhibit cell survival and induce cell apoptosis via regulating autophagy in PC cells. Further mechanistic study identified that miR-137 sensitized PANC-1 cells to Dox through inhibiting ATG5 and autophagy *in vitro* and *in vivo*.

Drug resistance is a hallmark of tumor, which contributes to relapse and poor prognosis (Sui et al., 2014). Increasing evidence showed that drug treatment induced autophagy and caused decrease in miRNAs in different cancers. For example, cisplatin treatment results in induction of autophagy and downregulation of miR-199a-5p (Xu et al., 2012). Dox triggered autophagy but reduced the level of miR-26a/b in HCC cells (Jin et al., 2017). MiR-137 has been reported to be a tumor suppressor miRNA in several solid tumors (Su et al., 2016). It has been showed that miR-137 played important roles in regulating cancer cell invasion, chemo-resistance and tumor growth of pancreatic cancer (Su et al., 2016). Previous studies demonstrated the decreased expression of miR-137 in pancreatic cancer (Chin et al., 2018; Ding et al., 2018). However, so far there were no reports demonstrated the regulation of miR-137 by Dox. In the current study, we found that Dox induced autophagy and decrease in the expression level of miR-137 in PC cells.

However, the function of the decreased expression of miR-137 is not clear. Previous study showed that miR-137 markedly inhibits mitochondrial degradation by autophagy without affecting global autophagy (Li et al., 2014). The role of autophagy in cell survival upon nutrient deprivation is context-dependent and complicated in normal cells. In line with the context dependent mechanism in normal cells, autophagy also plays dual and contradictory roles in cancer (Rubinsztein et al., 2007). It was reported that autophagy is required for tumorigenic growth of pancreatic cancers de novo (Huang et al., 2016). Furthermore, therapeutic treatment can induce autophagy in

pancreatic cancer, which seems to function as a protective cell survival mechanism (Zhu et al., 2018). Previous studies had demonstrated that miR-137 modulates drug sensitivity in several tumors (Shen et al., 2016; Takwi et al., 2014; Lu et al., 2017). Therefore, it can be inferred that autophagy may contributes to chemotherapeutic resistance and miR-137 is possible to enhance the drug activity via targeting autophagy. As expected, our findings showed that Dox treatment resulted in the increase in the autophagy activity while expression of miR-137 reversed the effect of Dox on the formation of autophagosomes. Overexpression of miR-137 dramatically sensitized the ability of Dox to induced cell apoptosis and inhibit cell survival via targeting autophagy. Increasing evidence suggests that miR-317 was able to regulate autophagy and drug resistance by directly binding to several targets (Li et al., 2014). ATG5 is an attractive target for inhibiting autophagy. For example, miRNA-181a inhibits autophagy by targeting ATG5 in hepatocellular carcinoma (Yang et al., 2018). miRNA-142-3p targets ATG5 to inactivate autophagy and sensitize hepatocellular carcinoma cells to sorafenib (Zhang et al., 2018b). By gain-of-function and loss-of-function studies, we demonstrated that miR-137 targeted the 3′UTR of ATG5 and negatively regulated ATG5 expression in PC cells, identifying ATG5 as a bona fide target of miR-137. Furthermore, restoration of miR-137 sensitized doxorubicin-resistant PC cells and significantly reduced the growth of doxorubicin-resistant neuroblastoma xenografts though targeting ATG5 *in vitro* and *in vivo*.

Here, it is the first time we have found that Dox decrease in the expression of miR-137 in PC cells. However, the mechanism for downregulation of miR-137 is unclear. We have investigated the result at the cellular and animal levels, but further studies on clinical samples are required. Moreover, though our results showed that miR-137 regulated autophagy through targeting ATG5 expression, intensive mechanistic study need to be implemented in the future. So in the future, we are going to overcome the attendant limitations of the present study.

5. Conclusions

In summary, our findings demonstrate that miR-137 is a crucial regulator of apoptosis by targeting ATG-5 which potentiate the cancer response to doxorubicin treatment, providing a novel cancer therapy strategy that combines the use of miR-137 with chemotherapy.

Conflict of interest

The authors declare that they have no conflict of interest.

Funding

This research did not receive any specific grant from funding agencies in the public, commercial, or not-for-profit sectors.

Acknowledgement

We would like to give our sincere gratitude to the reviewers for their constructive comments.

References

Chen, M.J., Wu, D.W., Wang, G.C., Wang, Y.C., Chen, C.Y., Lee, H., 2018. MicroRNA-630 may confer favorable cisplatin-based chemotherapy and clinical outcomes in non-small cell lung cancer by targeting Bcl-2. Oncotarget 9, 13758–13767.

Chin, V., Nagrial, A., Sjoquist, K., O'Connor, C.A., Chantrill, L., Biankin, A.V., Scholten, R.J., Yip, D., 2018. Chemotherapy and radiotherapy for advanced pancreatic cancer. Cochrane Database Syst. Rev. 3, CD011044.

Ding, F., Zhang, S., Gao, S., Shang, J., Li, Y., Cui, N., Zhao, Q., 2018. MiR-137 functions as a tumor suppressor in pancreatic cancer by targeting MRGBP. J. Cell. Biochem.

Gozuacik, D., Akkoc, Y., Ozturk, D.G., Kocak, M., 2017. Autophagy-regulating microRNAs and cancer. Front. Oncol. 7, 65.

Huang, Z., Zhou, L., Chen, Z., Nice, E.C., Huang, C., 2016. Stress management by autophagy: implications for chemoresistance. Int. J. Cancer 139, 23–32. https://doi.org/10.1002/ijc.29990.

Jin, F., Wang, Y., Li, M., Zhu, Y., Liang, H., Wang, C., Wang, F., Zhang, C.Y., Zen, K., Li, L., 2017. MiR-26 enhances chemosensitivity and promotes apoptosis of hepatocellular carcinoma cells through inhibiting autophagy. Cell Death Dis. 12 (1), e2540 8.

Levine, B., Kroemer, G., 2008. Autophagy in the pathogenesis of disease. Cell 132, 27–42.

Li, W., Zhang, X., Zhuang, H., Chen, H.G., Chen, Y., Tian, W., Wu, W., Li, Y., Wang, S., Zhang, L., Chen, Y., Li, L., Zhao, B., Sui, S., Hu, Z., Feng, D., 2014. MicroRNA-137 is a novel hypoxia-responsive microRNA that inhibits mitophagy via regulation of two mitophagy receptors FUNDC1 and NIX. J. Biol. Chem. 15, 10691–10701.

Li, D., Shan, W., Fang, Y., Wang, P., Li, J., 2017. miR-137 acts as a tumor suppressor via inhibiting CXCL12 in human glioblastoma. Oncotarget 8, 101262–101270.

Liu, X., Chen, X., Yu, X., Tao, Y., Bode, A.M., Dong, Z., Cao, Y., 2013. Regulation of microRNAs by epigenetics and their interplay involved in cancer. J. Exp. Clin. Cancer Res. 22, 32–96.

Lu, A.Q., Lv, B., Qiu, F., Wang, X.Y., Cao, X.H., 2017. Upregulation of miR-137 reverses sorafenib resistance and cancer-initiating cell phenotypes by degrading ANT2 in hepatocellular carcinoma. Oncol. Rep. 37, 2071–2078.

Min, A., Zhu, C., Peng, S., Rajthala, S., Costea, D.E., Sapkota, D., 2015. MicroRNAs as important players and biomarkers in oral carcinogenesis. Biomed Res. Int. 2015, 186904.

Neault, M., Mallette, F.A., Richard, S., 2016. miR-137 modulates a tumor suppressor network-inducing senescence in pancreatic cancer cells. Cell Rep. 14, 1966–1978.

Rosenberg, A., Mahalingam, D., 2018. Immunotherapy in pancreatic adenocarcinoma-overcoming barriers to response. J. Gastrointest. Oncol. 9, 143–159.

Rubinsztein, D.C., Gestwicki, J.E., Murphy, L.O., Klionsky, D.J., 2007. Potential therapeutic applications of autophagy. Nat. Rev. Drug Discov. 6, 304–312.

Ruocco, N., Costantini, S., Costantini, M., 2016. Blue-print autophagy: potential for cancer treatment. Mar. Drugs 14.

Sato-Dahlman, M., Wirth, K., Yamamoto, M., 2018. Role of gene therapy in pancreatic cancer-a review. Cancers (Basel) 10.

Shen, H., Wang, L., Ge, X., Jiang, C.F., Shi, Z.M., Li, D.M., Liu, W.T., Yu, X., Shu, Y.Q., 2016. MicroRNA-137 inhibits tumor growth and sensitizes chemosensitivity to paclitaxel and cisplatin in lung cancer. Oncotarget 7, 20728–20742.

Su, T.J., Ku, W.H., Chen, H.Y., Hsu, Y.C., Hong, Q.S., Chang, G.C., Yu, S.L., Chen, J.J., 2016. Oncogenic miR-137 contributes to cisplatin resistance via repressing CASP3 in lung adenocarcinoma. Am. J. Cancer Res. 6, 1317–1330.

Sui, H., Zhu, L., Deng, W., Li, Q., 2014. Epithelial-mesenchymal transition and drug resistance: role, molecular mechanisms, and therapeutic strategies. Oncol. Res. Treat. 37, 584–589.

Sun, F.D., Wang, P.C., Luan, R.L., Zou, S.H., Du, X., 2018. MicroRNA-574 enhances doxorubicin resistance through down-regulating SMAD4 in breast cancer cells. Eur. Rev. Med. Pharmacol. Sci. 22, 1342–1350.

Takwi, A.A., Wang, Y.M., Wu, J., Michaelis, M., Cinatl, J., Chen, T., 2014. miR-137 regulates the constitutive androstane receptor and modulates doxorubicin sensitivity in parental and doxorubicin-resistant neuroblastoma cells. Oncogene 33, 3717–3729.

Wiedmer, T., Blank, A., Pantasis, S., Normand, L., Bill, R., Krebs, P., Tschan, M.P., Marinoni, I., Perren, A., 2017. Autophagy inhibition improves sunitinib efficacy in pancreatic neuroendocrine tumors via a lysosome-dependent mechanism. Mol. Cancer Ther. 16, 2502–2515.

Xiao, J., Peng, F., Yu, C., Wang, M., Li, X., Li, Z., Jiang, J., Sun, C., 2014. microRNA-137 modulates pancreatic cancer cells tumor growth, invasion and sensitivity to chemotherapy. Int. J. Clin. Exp. Pathol. 7, 7442–7450.

Xu, N., Zhang, J., Shen, C., Luo, Y., Xia, L., Xue, F., Xia, Q., 2012. Cisplatin-induced downregulation of miR-199a-5p increases drug resistance by activating autophagy in HCC cell. Biochem. Biophys. Res. Commun. 423, 826–831.

Xu, X.D., Zhao, Y., Zhang, M., He, R.Z., Shi, X.H., Guo, X.J., Shi, C.J., Peng, F., Wang, M., Shen, M., Wang, X., Li, X., Qin, R.Y., 2017. Inhibition of autophagy by deguelin sensitizes pancreatic cancer cells to doxorubicin. Int. J. Mol. Sci. 18.

Yan, Y., Xu, Z., Dai, S., Qian, L., Sun, L., Gong, Z., 2016. Targeting autophagy to sensitive glioma to temozolomide treatment. J. Exp. Clin. Cancer Res. 2 (35), 23.

Yang, J., He, Y., Zhai, N., Ding, S., Li, J., Peng, Z., 2018. MicroRNA-181a inhibits autophagy by targeting Atg5 in hepatocellular carcinoma. Front. Biosci. (Landmark Ed) 23, 388–396.

Zeng, Y., Huo, G., Mo, Y., Wang, W., Chen, H., 2015. MIR137 Regulates Starvation-Induced Autophagy by Targeting ATG7. J. Mol. Neurosci. 4, 815–821.

Zhang, Y., Yang, C., Cheng, H., Fan, Z., Huang, Q., Lu, Y., Fan, K., Luo, G., Jin, K., Wang, Z., Liu, C., Yu, X., 2018a. Novel agents for pancreatic ductal adenocarcinoma: emerging therapeutics and future directions. J. Hematol. Oncol. 11, 14.

Zhang, K., Chen, J., Zhou, H., Chen, Y., Zhi, Y., Zhang, B., Chen, L., Chu, X., Wang, R., Zhang, C., 2018b. PU.1/microRNA-142-3p targets ATG5/ATG16L1 to inactivate autophagy and sensitize hepatocellular carcinoma cells to sorafenib. Cell Death Dis. 9, 312.

Zhu, J., Chen, Y., Ji, Y., Yu, Y., Jin, Y., Zhang, X., Zhou, J., 2018. Gemcitabine induces apoptosis and autophagy via the AMPK/mTOR signaling pathway in pancreatic cancer cells. Biotechnol. Appl. Biochem.